Published in final edited form as:
J Glaucoma. 2008 ; 17(7): 519–528. doi:10.1097/IJG.0b013e3181629a02.

Blood Vessel Contributions to Retinal Nerve Fiber Layer Thickness Profiles Measured With Optical Coherence Tomography

Donald C. Hood, PhD[*], **Brad Fortune, OD, PhD**[†], **Stella N. Arthur, MD**[‡], **Danli Xing, BA**[‡], **Jennifer A. Salant**[*], **Robert Ritch, MD**[‡,§], and **Jeffrey M. Liebmann, MD**[‡,‖,¶]

[*]Departments of Psychology and Ophthalmology, Columbia University, New York

[‡]New York Eye and Ear Infirmary, New York

[‖]New York University School of Medicine, New York

[¶]Manhattan Eye, Ear, and Throat Hospital, New York

[§]New York Medical College, Valhalla, NY

[†]Discoveries in Sight, Devers Eye Institute, Legacy Health System, Portland, OR

Abstract

Purpose—To understand better the influence of retinal blood vessels (BVs) on the interindividual variation in the retinal nerve fiber layer (RNFL) thickness measured with optical coherence tomography (OCT).

Subjects and Methods—RNFL thickness profiles were measured by OCT in 16 control individuals and 16 patients. The patients had advanced glaucoma defined by abnormal disc appearance, abnormal visual fields, and a mean visual field deviation worse than − 10 dB.

Results—In general, the OCT RNFL thickness profiles showed 4 local maxima, with the peak amplitudes in the superior and inferior regions occurring in the temporal (peripapillary) disc region. There was considerable variability among individuals in the location of these maxima. However, the 4 maxima typically fell on, or near, a major BV with the temporal and inferior peaks nearly always associated with the main temporal branches of the superior and inferior veins and arteries. In the patients' hemifields with severe loss (mean visual field deviation worse than − 20 dB), the signals associated with the major BVs were in the order of 100 to 150 μm.

Conclusions—The variation in the local peaks of the RNFL profiles of controls correlates well with the location of the main temporal branches of the superior and inferior veins and arteries. This correspondence is, in part, due to a direct BV contribution to the shape of the OCT RNFL and, in part, due to the fact that BVs develop along the densest regions of axons. Although the overall BV contribution was estimated to be relatively modest, roughly 13% of the total peripapillary RNFL thickness in controls, their contribution represents a substantial portion locally and increases in importance with disease progression.

Keywords

glaucoma; optical coherence tomography; neuroophthalmology

Reprints: Donald C. Hood, PhD, Department of Psychology, 406 Schermerhorn Hall, Columbia University, New York NY, 10027 (dch3@columbia.edu).

Various diseases, most notably glaucoma, result in the death of retinal ganglion cells (RGC) and the degeneration of their axons. The loss of RGC axons in turn leads to a thinning of the retinal nerve fiber layer (RNFL), the collection of axons lying just below the vitreoretinal interface. It is now possible to obtain a noninvasive measure of the thickness of the human RNFL layer with techniques such as optical coherence tomography (OCT).

OCT uses an interferometric method to determine the depth of surfaces differing in reflectance much in the way sonar or ultrasound works.[1–4] A computer algorithm then identifies the anterior and posterior boundaries of the highly reflective RNFL to provide an estimate of its thickness.[2,4] The images in Figure 1 were taken from a clinical report of RNFL thickness provided by a commercially available OCT instrument. The black curve in Figure 1A shows the RNFL thickness profile for an individual with normal vision and the green region shows the 95% confidence range for a group of normal controls. There is a prominent peak in the superior temporal (ST) (blue line in Fig. 1A) and in the inferior temporal (IT) (orange line) region of the disc. Most individuals also show secondary maxima positioned nasal to the 2 main peaks and indicated with the yellow and green lines in Figure 1A.

Although this pattern describes the general appearance of most RNFL thickness profiles from healthy eyes, there is considerable interindividual variation. Recently, Ghadiali et al[5] showed that although the RNFL profiles from the 2 eyes of an individual were very similar, the profiles differed markedly in both amplitude and waveform across individuals. Understanding the sources of this intersubject variability is central to the understanding and improvement of the OCT RNFL as a test for glaucomatous damage. In this study, we evaluate the influence that blood vessels (BVs) traveling within the RNFL have on the thickness profiles obtained by OCT and on the interindividual variation of those profiles.

BVs must influence the RNFL thickness measured with OCT. Retinal arteries coming from, and veins going to, the optic disc travel in the RNFL and contribute to its thickness (see, eg, Fig. 7 in Ref. 6, Fig. 3 in Ref., 7 and Fig. 2B in Ref. 8). In fact, the presence of these BVs can be inferred from the shadows they cast in OCT images. For example, it is well known that there are dark bands in the OCT scan due to shadows cast by BVs.3 Examples of these shadows can be seen in the scan in Figure 1B where their positions are indicated by red lines numbered 1 to 8. The location of these shadows is marked on the photograph of the optic disc in Figure 1C (red hash marks numbered 1 to 8). Notice that the shadows line up with the major BVs. Presumably, the BVs are contributing directly to the RNFL thickness in the locations associated with the shadows. The purpose of this study was to determine whether BVs influence the shape of the RNFL profiles measured by OCT, and thus also contribute to the interindividual variability of OCT RNFL thickness profiles.

To better understand how the distribution of BVs contribute to the variation in OCT RNFL profiles, OCT measurements were made on 16 controls with normal vision and 16 patients with advanced glaucoma. The patients with advanced glaucoma were studied to see the effects of the BVs when most of the RGC axons are presumed to be missing from the RNFL.

MATERIALS AND METHODS

Subjects

Sixteen healthy control individuals and 16 patients with advanced glaucoma were studied. All patients had glaucomatous discs (cupping, rim loss, hemorrhages, or RNFL defects) as evaluated with stereo photography. In addition, the inclusion criteria included visual acuity of 20/40 or better, < 5 D myopia or hyperopia, and reliable visual fields (ie, < 30% fixation losses, false negatives, or false positives) with mean deviations (MD) worse than − 10 dB. The mean

age of these 16 patients was 54.9 ± 10.4 years and the MD was − 17.3 ± 6.0 dB. The inclusion criteria for the 16 control individuals were visual acuity of 20/20 or better, < 5 D myopia or hyperopia, intraocular pressure ≤22 mm Hg, reliable and normal visual fields (pattern standard deviation and glaucoma hemifield test within normal limits), open angles on gonioscopy, and normal optic nerves (no evidence of cupping, rim loss, hemorrhages, or RNFL defects). The control group was matched to the patient group for race (black) and were similar in age (53.6 ± 8.2 y). All individuals had OCT tests within 6 months of the visual field. Procedures followed the tenets of the Declaration of Helsinki and the protocol was approved by the Institutional Board of Research Associates of Columbia University.

Testing

Visual field testing was performed using automated perimetry (Humphrey Field Analyzer, program 24-2 SITA-standard, Carl Zeiss Meditech, Dublin, CA).

The thickness of the peripapillary RNFL was measured with the Stratus OCT (Carl Zeiss Meditec Inc, Dublin, CA) using version 4.0 software and the fast scan protocol. All scans had a signal strength of ≥ 7 and were centered on the optic nerve. During a single recording, 3 scans are made around a ring 3.4 mm in diameter with a spatial resolution of 256 points and then averaged. The 256 OCT RNFL values for the RNFL profile were exported for each eye.

Scanning laser polarimetry (SLP) was also performed on all eyes using the GDx-VCC Nerve Fiber Layer Analyzer (Carl Zeiss Meditech, Dublin, CA).

Relating Location of Peaks of the OCT RNFL Profile to the Location of the BV

For most of the eyes, 4 local maxima were easily identified in the RNFL profile, 2 in the temporal region of the disc (0 to 90 degrees and 270 to 360 degrees) and 2 in the nasal region (90 to 270 degrees) as seen in Figure 2C, the RNFL thickness profile for one of the controls. For each of the 16 control eyes, these 4 local maxima in the RNFL profile were located and marked as indicated in Figure 2C with the colored vertical lines. In 2 eyes, a local maximum was not easily identified in the inferior nasal disc, that is, there was only 1 maximum in the inferior half of the disc (eg, Fig. 6B). The locations of the 4 maxima were recorded on the abscissa from 0 (temporal disc, 9 o'clock OD, and 3 o'clock OS) to 360 degrees (Fig. 2C). In addition, the peak (largest) RNFL thickness (arrows in Fig. 2C) was noted for the superior and inferior regions of the disc. (All eyes are shown as right eyes in the figures below.)

To relate the location of the maxima and peaks of the OCT RNFL profile to the location of the BVs, 2 procedures were employed. For procedure 1, the locations of the 4 maxima were marked on the fundus image from the SLP report (Fig. 2B) using a protractor. In Figure 2B, the green circle is the 3.4 mm diameter circle of the OCT scan (white circle in Fig. 2A) superimposed upon the SLP reflectance image. The SLP fundus image (Fig. 2B) was used in all cases for procedure 1, because the BVs were not clearly visible on some of the photos obtained with the OCT machine (Fig. 2A), as the bright flash was not always used. In the individuals with readable OCT photos, the locations of the local maxima relative to the BVs were similar to those for the SLP fundus image. In any case, a variety of factors will contribute to inaccuracies in locating the local maxima on the SLP reflectance image in Figure 2B, including subtle changes of eye position between the OCT scan and the OCT fundus photo, the centering of the eye, and the position and use of the protractor. However, our interest here is in the general agreement, or lack thereof, between the locations of the peaks and the locations of the BVs. The degree of precision of our technique is suited to this task as will be seen in the results in Figure 5B.

A second procedure provided a quantitative measure of the location of the ST and IT, veins (V), and arteries (A). These major branch BVs were identified on the SLP fundus image, as in Figure 2D, aided by a fundus photograph (Fig. 2E), which was available for all individuals in this study. A protractor was overlaid on the SLP fundus image and the locations of the 4 major BVs, as they crossed the scan line (green circle), were measured to the nearest degree. As with procedure 1 above, a variety of factors will influence these measurements, but again the level of precision here is sufficient to answer our questions.

Estimating the Contribution of the BVs

To obtain a rough estimate of the contribution of the ST and IT vein and artery to the OCT thickness, the results from the 16 patients with advanced glaucoma were examined. For inclusion, a hemifield had to satisfy the following criteria: the average visual field sensitivity loss (total deviation of all the points in the hemifield) had to be worse than − 20 dB and the SLP RNFL thickness had to be < 35 μm in the associated peripapillary region. Nine of the 16 eyes had at least 1 hemifield meeting these criteria; in 1 eye both hemifields met the criteria. Eight of these 10 hemifields were upper visual fields. Figure 3 shows an example in which the upper visual field (lower temporal disc) met the criteria. Figure 3B shows the total deviation values, whereas Figure 3F shows the RNFL profile for both the OCT (black) and SLP (red). The lower field/superior disc did not meet the SLP criterion. For the upper hemifield, which met the criteria, the ST or IT artery and vein were located on a single scan as shown by the blue (ITV) and pink (ITA) lines in Figure 3D. The signals from these veins and arteries were identified as the RNFL regions above the shadows nearest to the blue or pink line. The signals from all veins, and all but one of the arteries, in the 10 hemifields studied could be identified this way. To obtain an estimate of the thickness of these BVs in the anterior–posterior (*z*-axis) dimension, calibration rectangles of 3 sizes were used as shown in Figure 3C. These rectangles were placed on the single scan as in Figure 3D; whichever rectangle was filled by the BV in the horizontal dimension was recorded as the vertical BV diameter (ie, BVs were assumed to have round profiles). In this case (Fig. 3D), which was typical, the signals just filled the 150μm rectangle. The 100 μm was too small and the 175 μm too large. They are shown as the red rectangles in the inset to Figure 3D.

Quantification of Variation in RNLF Profiles

The OCT RNFL thickness profiles for the 16 controls were averaged to obtain a template RNFL profile. To quantify the degree of agreement between these RNFL profile templates and the RNFL thickness profile for each eye, a coefficient of determination R^2 was calculated for each eye. In particular,

$$R^2(\text{normalized}) = 1 - [\sum (X_i - T_i)^2 / \sum (X_i - \mu)^2]$$

where X_i is the individual's RNFL thickness at point i and μ the mean of this profile, $\Sigma(X_i/256)$. T_i is the thickness value of the template at point *i*. A coefficient of determination R^2 value of 1.0 indicates that the template can account for all the variance in the RNFL thickness. The R^2 values were also obtained after normalizing the thickness values by the average thickness value for each individual. In particular,

$$R^2(\text{normalized}) = 1 - [\sum (X_i/\mu - T_{n_i})^2 / \sum (X_i/\mu - 1)^2]$$

where T_n is the normalized template, that is, the mean of the 16 normalized RNFL profiles.

RESULTS

Variation in the Shape of the OCT RNFL Thickness Profile

Figure 4A shows the RNFL profiles from the 16 controls (gray curves) along with the mean of all 16, the group template (black curve). As previously reported,[5] there is considerable variation among controls in the shape of the RNFL profiles. The coefficient of determination, R^2, varied from 0.45 to 0.90, with a mean of 0.71 ± 0.13. That is, between 45% and 90% of the variance in an individual's RNFL profile could be accounted for by the group template. Figure 4B shows the same data normalized, that is, each RNFL profile was divided by its average thickness. This adjustment for overall amplitude only marginally decreased the variation among the controls, the average R^2 (normalized) was 0.74 ± 0.11 (range 0.51 to 0.92). Thus, the individual profiles varied in waveform independent of overall RNFL thickness. This variation can be seen in Figure 4C where the 6 profiles with the lowest R^2 (normalized) values are shown as the black curves with the group template from Figure 4B in gray.

Local Maxima in the OCT RNFL Profiles and BVs

To assess the relationship between the location of the BVs, 4 local maxima were identified in the RNFL profile. The locations of these maxima were marked on the SLP fundus image as shown in Figures 2B and D and described in the Methods. Notice that the 4 local maxima in Figure 2C fall on, or just adjacent to, major BVs. For example, by comparing Figures 2B and D, it is apparent that the ST maximum (blue line at 73 degrees in Fig. 2D) fell between the STA and STV, whereas the IT maximum (orange line at 290 degree in Fig. 2D) fell on the ITA.

For the 16 control eyes, the location of the maxima in the ST and IT regions of the disc (blue and orange lines in Fig. 2C) fell on a major BV for 22 of the 32 maxima (16 eyes and 2 maxima), and within 3 degrees of a major BV in 8 of the remaining 10 cases. In 2 cases, the local maxima in the temporal disc fell more than 5 degrees from a major BV. For the local maxima in the nasal disc (green and yellow lines in Fig. 2C), the local maxima fell on or within 3 degrees of a major BV in 29 of 32 cases. A local maximum was not easily identified in the inferior nasal disc of 2 individuals (see solid black curve in the left column of Fig. 6B). In 1 case, the local nasal maximum was about 7 degrees from a major BV. Although there were a few exceptions, in general, the local maxima occurred on or near a major BV.

To obtain a more precise quantification of this agreement, procedure 2 (see Methods) was used, whereby the locations of the STA and STV were measured and compared with the location of the peak RNFL thickness in the superior region of the disc. Here, "peak RNFL thickness" means the maximum thickness for the superior disc (ie, the larger of the 2 local maxima marked by blue and green). A similar analysis was carried out for the locations of the ITA and ITV and the peak RNFL thickness in the inferior disc (ie, the larger of the 2 local maxima marked by yellow and orange). For the example in Figure 2, the STV and STA were located at 71 and 80 degrees (Fig. 2D), whereas the superior peak of the RNFL profile (Fig. 2C) fell between them at 73.1 degrees. The ITV and ITA were located at 280 and 289 degrees (Fig. 2D), whereas the inferior peak of the RNFL profile (Fig. 2C) fell at 289.7 degrees, essentially on the ITA.

For all 16 controls, the average (± SD) location of these BVs was at 79.8 ± 12.6 degrees (STV), 82.0 ± 12.6° (STA), 271.9 ± 11.1 degrees (ITV) and 281.9 ± 7.0 degrees (ITA). Figure 5B shows a plot of the location of the ST and IT arteries (filled red symbols) and veins (filled blue symbols). The locations, in degrees, of the peak (ie, largest) RNFL thickness in the superior and inferior fields (*x*-axis) for each of the 16 controls (*y*-axis) are shown as the open circles. For all individuals, the peak in the inferior region of the disc occurred close to the ITA and/or ITV. The mean location of the IT peak was at 280.9 degrees, between the mean locations of

the ITV (271.9 degrees) and ITA (281.9 degrees), but closer, on average, to the ITA. The situation for the ST peak is a little more complicated. Although 13 of the peaks in the ST disc fell close to the STV and/or STA, 3 individuals (see circles with arrows) showed peaks more than 30 degrees to the nasal side of the STV/STA. The RNFL profiles for these 3 are shown as the black curve in the first column of Figures 6B–D. For comparison, the profile for the more typical case, from Figure 2, is presented in Figure 6A and the profile for an individual whose peak amplitude in the superior disc fell to the temporal side of the group template is shown in Figure 6E. The dashed black curve in the left column is the group template. Notice that in the case of the RNFL profiles in Figures 6B–D (left column), the peak RNFL thickness in the superior disc is not the first local maxima. The RNFL profiles of the other 13 individuals resemble Figures 6A and E, in which the first prominent maxima is also the largest (peak) thickness in the superior disc. In Figures 6B and D, the peak thickness is associated with the second local maxima and the major artery and/or vein in the nasal, not temporal disc, as indicated by the green bar in the middle column of Figure 6. The first local maximum, however, is still associated with the STV and/or STA in these individuals. The + symbols at the end of the arrows in Figure 5B indicate the locations of the first maximum, as opposed to the largest peak. The mean location of all 16 first local maxima was at 78.7 degrees close to the mean locations of the STV (79.8 degrees) and STA (82.0 degrees).

Estimating the Contribution of the BVs to the OCT RNFL Thickness Profile

OCT signals associated with the ST and/or IT veins and arteries could be identified in those hemifields with severe field loss (see Methods). Figure 3 supplies an example. The ITA and ITV are shown as the pink and blue bars on Figures 3A and E. The location of these BVs are indicated on the single OCT scan in Figure 3D. The enhanced signal near these bars, and immediately above the nearest shadows, were assumed to be due to these BVs. The smallest of the 3 rectangles that is filled by these signals has a height of 150 μm. For the 10 hemifields meeting the criteria for a severely abnormal field and minimal SLP profile (see Methods), the OCT signals associated with the TA filled the 150-μm rectangle in 7 cases; filled the 100-μm rectangle in 1 case; failed to fill the smallest 100-μm, rectangle in 1 case; and in 1 case the associated shadow and signal could not be identified. The signals associated with the TVs were slightly larger, 8 filled the 150-μm rectangle and 2 filled the 100-μm rectangle.

It is also worth noting that the delineation algorithm often discounts BVs either partially or entirely, and thus the RNFL thickness estimate in regions associated with severe field losses sometimes does not include BV thicknesses. For example, in Figure 3D, the algorithm does not include the full thickness due to both the STA/STV (arrows) and the ITA/ITV (bars). However, this was not always the case as illustrated in Figure 3H. This is another single scan from the same OCT test. In the inset to Figure 3D, distinct signals from 3 BVs can be seen in the inferior peripapillary region, whereas in Figure 3H these signals are less distinct and the algorithm included them within the white lines.

DISCUSSION

The RNFL thickness profiles measured with OCT vary across individuals, even when refractive error and scan quality are taken into consideration.[5] This variation in RNFL profiles is large relative to that found owing to measurement error,[9–11] age,[12,13] or the size of the optic disc.[12,14] The results of the present study suggest that the location of the major temporal BVs can help us understand this variation. In particular, the location of the major temporal BVs is a good predictor of the location of the major maxima in the RNFL profile (Fig. 5B). There are 2 factors contributing to this correspondence. First, the BVs make a direct contribution to the OCT RNFL thickness. Second, the arcuate fiber bundles, providing the major contribution to the maxima, tend to travel with the major temporal BVs. These 2 factors are considered below.

First, consider the major BVs direct contribution to the RNFL thickness. The results from the patients with advanced glaucoma suggest that the contribution to the RNFL thickness from the ST and IT arteries and veins is, in general, about 100 to 150 μm, consistent with previous measurements of BV thickness.[15] Although there is some evidence that the size of the BVs decreases in patients with glaucoma,[16,17] this shrinkage is relatively small, about 15% of diameter,[16] and well within our error of measurement. In any case, given that the peak amplitudes of the average of the RNFL profiles (template in Fig. 4A) were 144.4 and 157.6 μm for the superior and inferior peaks, our estimate of 100 to 150 μm represents a sizable contribution to the RNFL thickness. Thus, it is not surprising that the location of the peaks in the RNFL profiles is associated with the location of major BVs, typically the ST and IT veins and/or arteries (Fig. 5B). Further, as the distribution of the BVs differs among healthy individuals, the signals due directly to the BVs undoubtedly contribute to the considerable variability in the shape of the RNFL profiles among controls.

However, the BVs per se account for a relatively small portion of the overall RNFL area measured with OCT near the optic disc in controls. A rough estimate can be obtained by assuming that there are 8 major arteries and veins, each having a diameter of 150 μm, and that the average total RNFL thickness from control eye scans is about 100 μm. This probably overestimates the thickness of many of these 8 BVs, but there are smaller BVs that are not included in the estimate. Using this rough approximation, about 13% of the overall OCT measured RNFL area is due directly to signals from the BVs. Although this contribution is relatively modest in controls, BVs can make a significant contribution in patients giving a false impression of the functional thickness remaining.

There is a second factor contributing to the correspondence between the location of the major temporal BVs and the maxima in the OCT RNFL thickness. In particular, because the development of the BVs is influenced by the axonal distribution,[18–20] one should expect some correlation between the location of the ST and IT arteries and veins, for example, and the shape of the distribution of RGC axons. In other words, the location of the BVs may help predict the variations in the profiles of OCT RNFL thickness because they mark regions of increased axonal density.

However, undoubtedly the location of the major temporal BVs will not explain all the variation in individual OCT RNFL profiles. It is likely that considerable intersubject variability exists in how well coupled axon density is to the location of the superior and inferior TA and TV. The SLP density plots in Figure 6 (third column) provide some evidence for this view. The red and yellow regions show the highest birefringence detected by measuring the retardance of polarized light by the RNFL. Although the SLP instrument converts retardance to an estimate of RNFL thickness by assuming a constant factor of 0.67 nm/μm, there is considerable evidence that this factor varies with location around the optic disc.[8,21–24] In any case, let us make a weaker assumption that the signal appearing as the arcuate bundle in Figure 6 (right column) is providing a reasonable indication of the location of the axons that make up this bundle. That is, assume that the bands of heightened signal in Figure 6 (right column) show the locations of the arcuate bundles of axons. Typically, the highest retardance measured by the SLP adjacent to the superior disc border falls around the STA and STV (see right column of Figs. 6A, B, E). However, for the individuals in Figures 6C and D, the SLP signal is greatest around the BVs in the superior nasal region. These seem to be examples of what Colen and Lemij[25] called split nerve fiber layer bundles. Histologic measurements of the monkey[8] and human RNFL[26,27] suggest that the peak thickness in the superior pole is not infrequently located nasal to the vertical meridian.

There is another factor that can influence the intersubject variability of the OCT RNFL profile, namely the algorithm used to define the RNFL thickness. This algorithm involves a fair amount

of spatial averaging. A local, large contribution from a BV is likely to be ignored by the algorithm, that is, fall, in part, outside the white boundaries, especially in regions with extensive damage. On the other hand, 2 or more BVs, or a BV with a large contribution from neighboring axons, will be included inside the white boundaries set by the algorithm. This contribution of the algorithm to intersubject variability is probably relatively small for healthy individuals, but it can be quit large for patients with severe axonal loss as illustrated in Figure 3H.

To summarize, in general, the OCT RNFL profiles show 4 local maxima with the maxima in the temporal region of the disc typically being the larger of the 2 superior or inferior maxima (Fig. 2C). These local maxima are typically associated with BVs for 2 reasons. First, the BVs make a direct contribution to the RNFL thickness. Second, the axonal portion of the RNFL is probably thickest in the region of the BVs, in most individuals in the regions of the ST and IT arteries and veins. Although the direct contribution of BVs to RNFL may be relatively minor in controls, it can have a relatively large influence in patients with significant field loss. Finally, a better understanding of the relationship between the distribution of the major BVs and the OCT RNFL thickness might lead to an improvement in the specificity of the OCT RNFL test. In principle, it may be possible to decrease the variability in OCT tests by comparing patients and controls with similar distributions of BVs.

Acknowledgments

Supported by National Eye Institute Grants U10-EY-14267, R01-EY-09076 and RO1-EY-02115, the Ephraim and Catherine Gildor Research Fund of the New York Glaucoma Research Institute.

REFERENCES

1. Huang D, Swanson EA, Lin CP, et al. Optical coherence tomography. Science 1991;254:1178–1181. [PubMed: 1957169]
2. Schuman JS, Hee MR, Puliafito CA, et al. Quantification of nerve fiber layer thickness in normal and glaucomatous eyes using optical coherence tomography. Arch Ophthalmol 1995;113:586–596. [PubMed: 7748128]
3. Fujimoto, JG.; Hee, MR.; Huang, D., et al. Principles of optical coherence tomography. In: Schuman, JS.; Puliafito, CA.; Fujimoto, JG., editors. Optical Coherence Tomography of Ocular Diseases. NJ: Slack Inc; 2004.
4. Hee, MR.; Fujimoto, JG.; Ko, T., et al. Interpretation of the optical coherence tomography image. In: Schuman, JS.; Puliafito, CA.; Fujimoto, JG., editors. Optical Coherence Tomography of Ocular Diseases. NJ: Slack Inc; 2004.
5. Ghadiali Q, Hood DC, Lee C, et al. An analysis of normal variations in retinal nerve fiber layer thickness profiles measured with optical coherence tomography. 2007 In press.
6. Radius RL. Thickness of the retinal nerve fiber layer in primate eyes. Arch Ophthalmol 1980;98:1625–1629. [PubMed: 6775622]
7. Quigley HA, Addicks EM. Quantitative studies of retinal nerve fiber layer defects. Arch Ophthalmol 1982;100:807–814. [PubMed: 7082210]
8. Morgan JE, Waldock A, Jeffery G, et al. Retinal nerve fibre layer polarimetry: histological and clinical comparison. Br J Ophthalmol 1998;82:684–690. [PubMed: 9797673]
9. Blumenthal EZ, Williams JM, Weinreb RN, et al. Reproducibility of nerve fiber layer thickness measurements by use of optical coherence tomography. Ophthalmology 2000;107:2278–2282. [PubMed: 11097610]
10. Paunescu LA, Schuman JS, Price LL, et al. Reproducibility of nerve fiber thickness, macular thickness, and optical nerve head measurements using StratusOCT. Invest Ophthalmol Vis Sci 2004;45:1716–1724. [PubMed: 15161831]
11. Budenz DL, Chang RT, Huang X, et al. Reproducibility of retinal nerve fiber thickness measurements using the stratus OCT in normal and glaucomatous eyes. Invest Ophthalmol Vis Sci 2005;46:2440–2443. [PubMed: 15980233]

12. Bowd C, Zangwill LM, Blumenthal EZ, et al. Imaging of the optic disc and retinal nerve fiber layer: the effects of age, optic disc area, refractive error, and gender. J Opt Soc Am A Opt Image Sci Vis 2002;19:197–207. [PubMed: 11778725]
13. Hougaard JL, Ostenfeld C, Heijl A, et al. Modelling the normal retinal nerve fibre layer thickness as measured by Stratus optical coherence tomography. Graefes Arch Clin Exp Ophthalmol 2006;244:1607–1614. [PubMed: 16788824]
14. Savini G, Zanini M, Carelli V, et al. Correlation between retinal nerve fibre layer thickness and optic nerve head size: an optical coherence tomography study. Br J Ophthalmol 2005;89:489–492. [PubMed: 15774930]
15. Jonas JB, Nguyen NX, Naumann GO. The retinal nerve fiber layer in normal eyes. Ophthalmology 1989;96:627–632. [PubMed: 2748120]
16. Jonas JB, Fernandez MC, Naumann GO. Parapapillary atrophy and retinal vessel diameter in nonglaucomatous optic nerve damage. Invest Ophthalmol Vis Sci 1991;32:2942–2947. [PubMed: 1917397]
17. Rader J, Feuer WJ, Anderson DR. Peripapillary vasoconstriction in the glaucomas and the anterior ischemic optic neuropathies. Am J Ophthalmol 1994;117:72–80. [PubMed: 8291596]
18. Miller G. Nerves tell arteries to make like a tree. Science 2002;296:2121–2122. [PubMed: 12077377]
19. Carmeliet P, Tessier-Lavigne M. Common mechanisms of nerve and blood vessel wiring. Nature 2005;436:193–200. [PubMed: 16015319]
20. Dorrell MI, Friedlander M. Mechanisms of endothelial cell guidance and vascular patterning in the developing mouse retina. Prog Retin Eye Res 2006;25:277–295. [PubMed: 16515881]
21. Cense B, Chen TC, Park BH, et al. Thickness and birefringence of healthy retinal nerve fiber layer tissue measured with polarization-sensitive optical coherence tomography. Invest Ophthalmol Vis Sci 2004;45:2606–2612. [PubMed: 15277483]
22. Huang XR, Bagga H, Greenfield DS, et al. Variation of peripapillary retinal nerve fiber layer birefringence in normal human subjects. Invest Ophthalmol Vis Sci 2004;45:3073–3080. [PubMed: 15326123]
23. Rylander HG III, Kemp NJ, Park J, et al. Birefringence of the primate retinal nerve fiber layer. Exp Eye Res 2005;81:81–89. [PubMed: 15978258]
24. Cense B, Mujat M, Chen TC, et al. Polarization-sensitive spectral-domain optical coherence tomography using a single line scan camera. Optics Express 2007;15:2421–2431. [PubMed: 19532479]
25. Colen TP, Lemij HG. Prevalence of split nerve fiber layer bundles in healthy eyes imaged with scanning laser polarimetry. Ophthalmology 2001;108:151–156. [PubMed: 11150281]
26. Varma R, Skaf M, Barron E. Retinal nerve fiber layer thickness in normal human eyes. Ophthalmology 1996;103:2114–2119. [PubMed: 9003346]
27. Dichtl A, Jonas JB, Naumann GO. Retinal nerve fiber layer thickness in human eyes. Graefes Arch Clin Exp Ophthalmol 1999;237:474–479. [PubMed: 10379607]

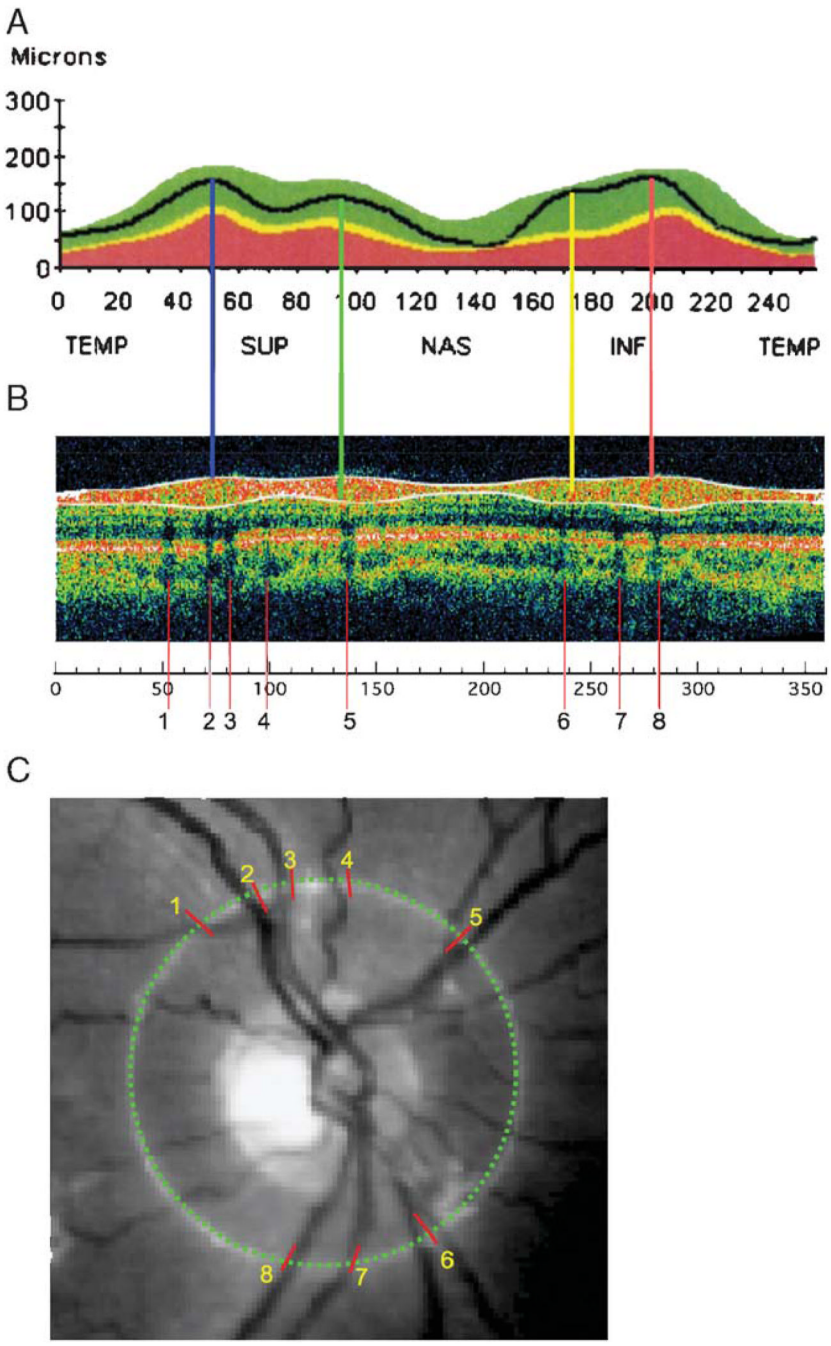

FIGURE 1.

The RNFL profile (A), scan density (B), and fundus image (C) from the OCT RNFL report of a commercial instrument. The colored vertical lines in (A) mark the location of the local maxima of the RNFL profile. The shadows in (B) are marked with vertical red lines. The locations of these red lines were measured on the scale in (B) and these locations were transferred to the image in (C) using a protractor.

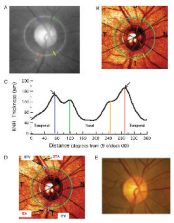

FIGURE 2.
The colored vertical lines in (B) mark the location of the local maxima of the RNFL profile from one of the control individuals. The locations of these lines were noted on the scale in (C) and these locations were transferred to the fundus images in (A) and (B) using a protractor. The locations of the STA and STV and the ITA and ITV are shown in (D). Veins and arteries were located with the aid of a fundus photograph (E).

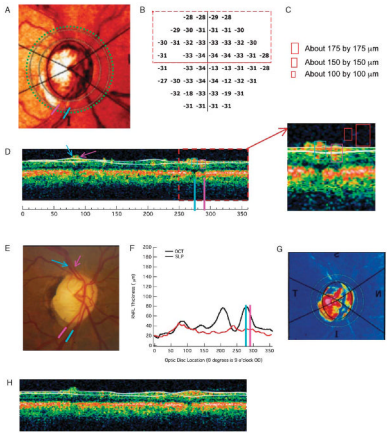

FIGURE 3.

OCT and SLP results for a patient with advanced glaucoma that illustrate the influence of the blood vessels on the OCT RNFL profile. A, Image of optic disc with circle of analysis and ITV (blue) and ITA (pink) indicated. B, Total deviation visual field plot. C, Calibration rectangles. D, Single OCT scan with ITV (blue) and ITA (pink) indicated. E, Image of disc showing STV/A (arrows) and ITV/A (lines). F, RNFL files for OCT and SLP. G, SLP density plot. H, Single OCT scan during same run as D. See text for details.

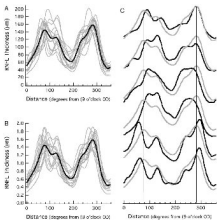

FIGURE 4.

A, The OCT RNFL thickness profiles from 16 controls (gray) with the mean of these 16 profiles (black). B, The RNFL profiles in (A) normalized by dividing each by its mean RNFL thickness. C, The OCT RNFL profiles from the 6 controls (black) with the largest R^2 values with the mean of all 16 control profiles (gray).

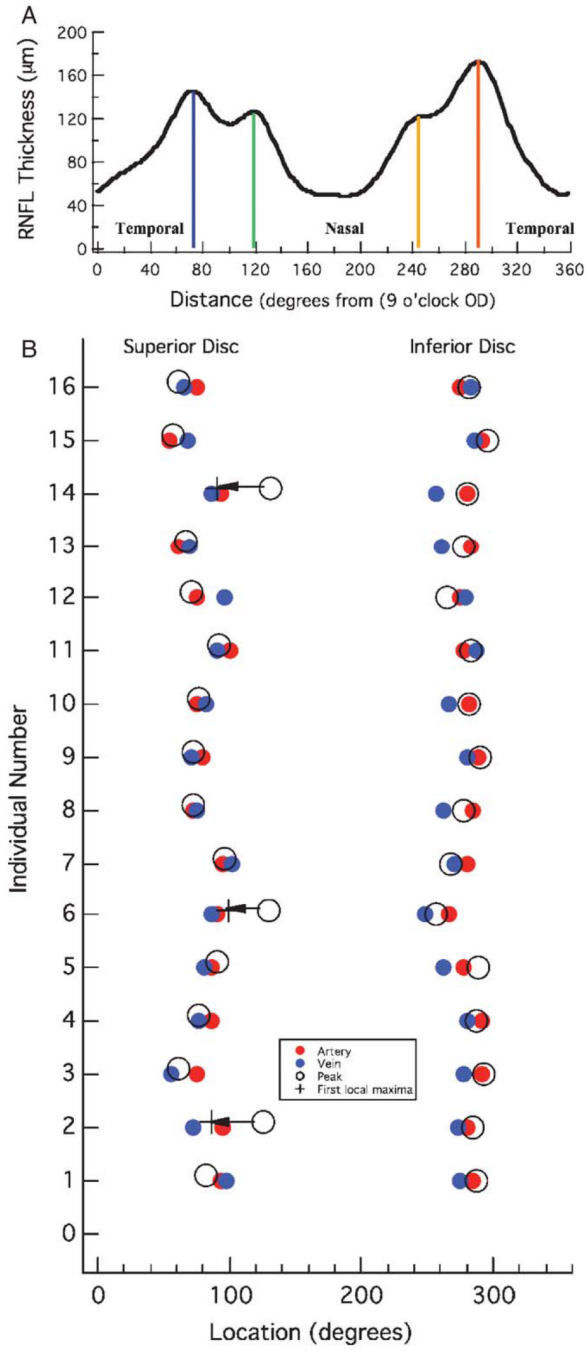

FIGURE 5.

A, The RNFL thickness profile from Figure 2C. B, The locations of the ST and IT arteries (red) and veins (blue) are shown with the locations of the peak response (open circles) for each of the 16 controls. The open circles with the arrow indicate the 3 individuals for whom the peak response coincided with the second local maxima rather than the first. The "+" symbol indicates the location of the local maxima in the ST region.

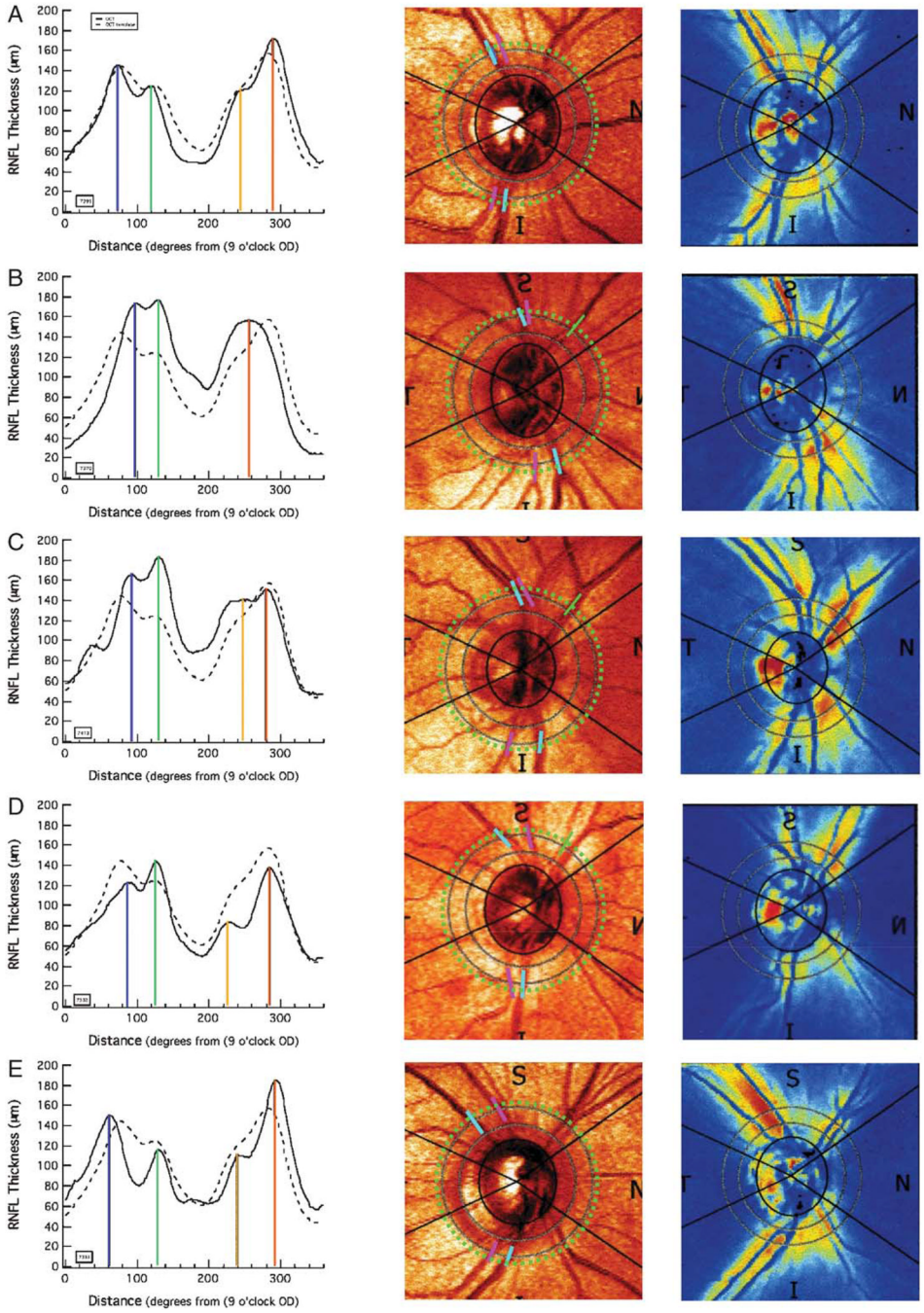

FIGURE 6.

Each row (A–E) shows the OCT and SLP results for a single control. The left column shows the OCT RNFL profiles for the individual (solid) along with the mean (dashed) for all 16 controls. The center column is the fundus image from the SLP scan with the ST and IT arteries (pink) and veins (blue) marked as they cross the scan circle (dotted green) of the OCT scan. The right column shows the density image for the individual's SLP scan. The individuals shown in panels B, C, and D correspond to individuals 6, 14, and 2 in Figure 5.